BİTLİS EREN ÜNİVERSİTESİ
FEN BİLİMLERİ DERGİSİ

ISSN: 2147-3129 / e-ISSN: 2147-3188

Article Type : Research Article
Received : May 28, 2025
Revised : October 5, 2025
Accepted : October 6, 2025
DOI : 10.17798/bitlisfen.1708528

Year : 2025
Volume : 14
Issue : 4
Pages : 2137-2154

DESIGN AND ANALYSIS OF LUENBERGER OBSERVER WITH AGGRESSIVE POLE PLACEMENT FOR BUCK CONVERTER

Fatih EVRAN [1]

Düzce University, Electrical and Electronics Engineering Department, Düzce, Türkiye, fatihevran@duzce.edu.tr

ABSTRACT

This study presents the design and analysis of a Luenberger observer with aggressively placed poles for a buck DC–DC converter. The objective is to estimate the inductor current and output voltage using only the measured output voltage, thereby enabling state feedback control in systems where current sensing is impractical or costly. A state-space model of the converter is derived, and the observer poles are placed sufficiently far in the left-half plane to ensure rapid estimation-error decay while maintaining numerical robustness. To validate the performance of the observer, MATLAB simulations are conducted under both nominal conditions and step changes in load and input voltage. Even when faced with abrupt disturbances, the results demonstrate that the proposed observer accurately reconstructs the unmeasured state variables with minimal delay, highlighting its robust performance. This makes the proposed observer a promising approach for advanced control schemes where full state feedback is essential.

Keywords: Luenberger observer, Buck dc-dc converter, Average state-space equation, State estimation.

1 INTRODUCTION

The rapid advancement of energy conversion technologies has accelerated the adoption of DC–DC converters across diverse applications, including photovoltaic systems, electric vehicles, portable electronics, and industrial power supplies [1–3]. These converters, operating at high switching frequencies and exhibiting inherently nonlinear dynamics, require accurate modeling and robust control strategies to ensure high efficiency, compact design, and fast transient responses. The performance of any control system therefore hinges on precise

License: CC BY-NC 4.0

representation of the converter's internal dynamics and effective observation of its internal states.

State-space modeling and control have gained prominence due to their ability to describe system dynamics in a matrix-based framework, enabling multivariable control design and direct integration of internal variables (such as inductor current and capacitor voltage) into the control law. Classical controllers such as proportional–integral (PI) and proportional–integral–derivative (PID) regulators are widely used in state-space settings and typically designed using pole placement or coefficient-matching methods [4, 5]. However, these methods can fall short in complex or time-varying systems, motivating advanced strategies such as Sliding Mode Control (SMC), noted for robustness to parameter variations and disturbances [6–10], and One-Cycle Control (OCC), recognized for cycle-by-cycle regulation accuracy [11]. Intelligent methods such as Fuzzy Logic Control and Artificial Neural Networks (ANNs) have also been applied to nonlinear or poorly modeled systems [12, 13]. More recently, Model Predictive Control (MPC) has attracted attention for handling multivariable constraints and optimizing performance over a finite prediction horizon [14, 15].

Despite these advances, many control strategies rely on internal state measurements, particularly inductor current and capacitor voltage, which are often difficult or costly to measure directly. To address this, observers are employed to estimate unmeasured states, providing reliable feedback for implementation. Observers can also be embedded in real-time simulation and Hardware-in-the-Loop (HIL) platforms, enabling rapid prototyping and validation of control schemes [16].

Several observer types are available, including the Luenberger observer [17–21], Sliding Mode observer [22, 23], and Extended Kalman Filter [24–26], each suited to specific system requirements. The Luenberger observer is especially attractive for linear systems due to its simplicity, predictable performance, and ease of implementation. By placing the observer poles well into the left half-plane (LHP), rapid exponential decay of the estimation error can be achieved, enabling accurate state reconstruction from output measurements alone. This, in turn, facilitates advanced controllers without additional physical sensors.

This study proposes a cost-effective alternative to direct inductor-current sensing in DC–DC converters by employing a Luenberger observer with aggressively placed poles. While conventional designs often prioritize stability via conservative pole locations, this work examines the trade-off between convergence speed and robustness by placing poles deeper in

the LHP. In particular, the influence of mismatched initial conditions is analyzed, showing that aggressive pole placement significantly reduces convergence time and settling time compared with conventional strategies.

The case study focuses on a PWM-based buck converter operating in Continuous Conduction Mode (CCM). The converter is modeled in state-space form, and the Luenberger observer estimates the inductor current using the duty ratio, the measured output and the input voltages. The performance of the observer (convergence speed, estimation accuracy, and dynamic behavior) is evaluated through MATLAB/Simulink simulations. Unlike many prior works emphasizing controller design, this study highlights observer development as a robust, accurate, and practical component for integration into advanced control frameworks, including real-time simulation and HIL applications.

The remainder of this paper is structured as follows: Section 2 presents the mathematical model of the buck converter in CCM. Section 3 outlines state estimation principles using the Luenberger observer. Section 4 details the observer design methodology. Section 5 discusses MATLAB-based simulation results, and Section 6 concludes with the main findings and perspectives.

2 MATHEMATICAL ANALYSIS OF THE BUCK CONVERTER

The buck converter steps down a higher input voltage v_{in} to a regulated lower output voltage v_{out}. The topology in Figure 1(a) comprises a controlled switch (MOSFET, *M*), a diode (*Q*), an inductor (*L*), a capacitor (*C*), and a load resistor (*R*). The inductor, capacitor, and load currents are i_L, i_c, and i_{out}, respectively.

Upon application of the gate signal in Figure 1(b), the MOSFET conducts over the interval $[0, dT_s]$ and the diode is reverse-biased, as illustrated in Figure 1(c). The ON-state dynamics are given by:

$$\begin{bmatrix} \frac{di_L}{dt} \\ \frac{dv_{out}}{dt} \end{bmatrix} = \underbrace{\begin{bmatrix} 0 & -\frac{1}{L} \\ \frac{1}{C} & -\frac{1}{RC} \end{bmatrix}}_{A_{on}} \begin{bmatrix} i_L \\ v_{out} \end{bmatrix} + \underbrace{\begin{bmatrix} \frac{1}{L} \\ 0 \end{bmatrix}}_{B_{on}} v_{in} \tag{1}$$

where $x = [i_L \quad v_{out}]^T$ is the state and $y = v_{out}$ is the measured output.

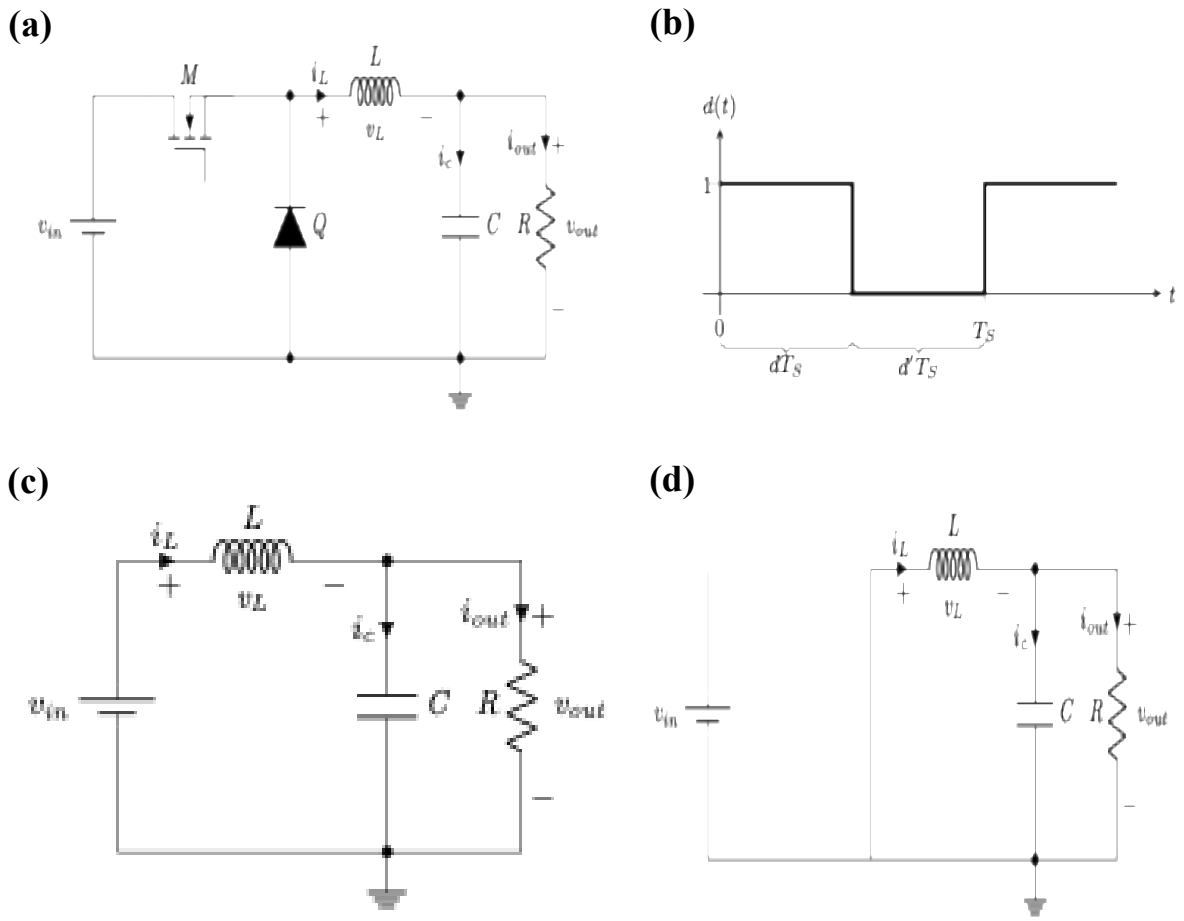


Figure 1. (a) The Circuit schematic of buck converter; (b) The switch control signal; (c) Equivalent circuit for $0 < t < dT_s$; (d) Equivalent circuit for $dT_s < t < T_s$.

For the OFF-state, the equivalent circuit in Figure 1(d) describes the dynamics as:

$$\begin{bmatrix} \frac{di_L}{dt} \\ \frac{dv_{out}}{dt} \end{bmatrix} = \underbrace{\begin{bmatrix} 0 & -\frac{1}{L} \\ \frac{1}{C} & -\frac{1}{RC} \end{bmatrix}}_{A_{off}} \begin{bmatrix} i_L \\ v_{out} \end{bmatrix} + \underbrace{\begin{bmatrix} 0 \\ 0 \end{bmatrix}}_{B_{off}} v_{in} \tag{2}$$

Averaging the ON and OFF dynamics over one switching period with the duty ratio d yields:

$$\frac{di_L}{dt} = -\frac{1}{L} v_{out} + \frac{d}{L} v_{in} \tag{3}$$

$$\frac{dv_{out}}{dt} = \frac{1}{C} i_L - \frac{1}{RC} v_{out} \tag{4}$$

For completeness, the duty ratio is defined explicitly as:

$$d = \frac{T_{on}}{T_s} \tag{5}$$

where T_{on} is the switch on-time, and T_s is the switching period. Using the time-averaged state-space representation and defining the known input as $u = d$, the averaged plant model can be written compactly as:

$$\dot{x} = Ax + Bu, \qquad y = Cx \tag{6}$$

where the system matrices are:

$$A = \begin{bmatrix} 0 & -\frac{1}{L} \\ \frac{1}{C} & -\frac{1}{RC} \end{bmatrix}, \qquad B = \begin{bmatrix} \frac{v_{in}}{L} \\ 0 \end{bmatrix}, \qquad C = [0\ 1] \tag{7}$$

In steady-state CCM, volt–second balance enforces zero average inductor voltage over one switching period, yielding the steady-state output voltage as:

$$V_o = DV_{in} \tag{8}$$

where D is the steady-state duty ratio. To ensure CCM operation, the inductance must satisfy:

$$L_{min} = \frac{(1-D)RT_s}{2} \tag{9}$$

3 STATE ESTIMATION USING A LUENBERGER OBSERVER

As illustrated in Figure 2, an observer reconstructs the state vector x from the known input u and the measured output y. Using the plant model in (6), the full-order Luenberger observer depicted in Figure 3 is defined by the following equation:

$$\dot{\hat{x}} = A\hat{x} + Bu + L_o(y - \hat{y}) = A\hat{x} + Bu + L_o(y - C\hat{x}), \qquad \dot{\hat{x}}(0) = \hat{x}_0 \tag{10}$$

with $\hat{y} = C\hat{x}$ and gain matrix L_o. Defining the estimation error as $e = x - \hat{x}$, the error dynamics become:

$$\dot{e} = \dot{x} - \dot{\hat{x}} = Ax + Bu - \left(A\hat{x} + Bu + L_o(y - C\hat{x})\right) = (A - L_oC)e, \qquad e(0) = e_0 \tag{11}$$

Thus, the observer converges exponentially if $A - L_oC$ is Hurwitz (i.e., all eigenvalues have negative real parts). The observer gain matrix L_o is chosen to place the eigenvalues of $A - L_oC$ to meet the desired speed and robustness criteria, assuming the pair (A, C) is observable.

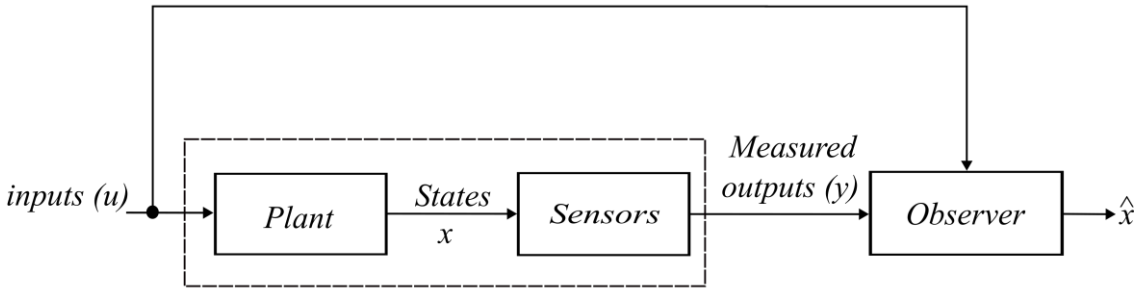


Figure 2. Schematic representation of plant-observer interconnection.

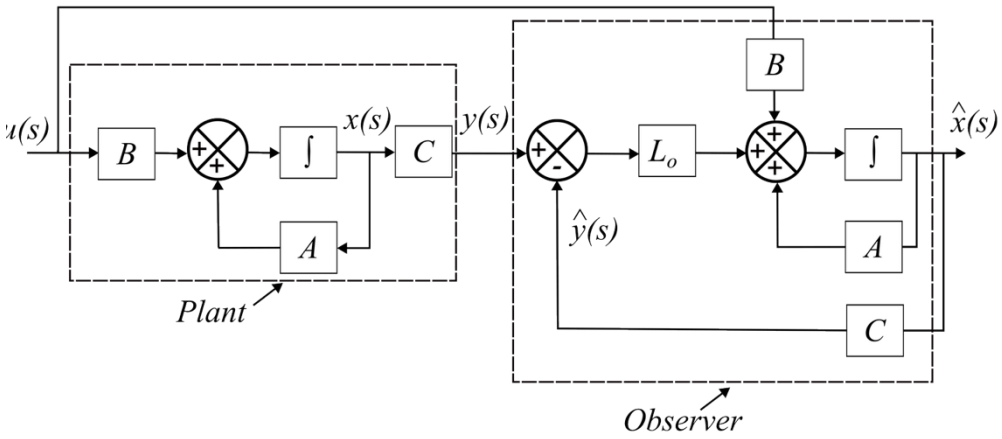


Figure 3. Block diagram of the plant with Luenberger observer.

To quantitatively evaluate the convergence performance of the Luenberger observer, a relative error-based threshold is adopted. Specifically, the convergence of each estimated state variable $\hat{x}$ to its true value x is defined in terms of the normalized absolute estimation error ϵ as follows:

$$\epsilon = \frac{|x - \hat{x}|}{|x|} \tag{12}$$

The observer is considered to have successfully converged when the relative estimation error remains below a predefined tolerance for all subsequent time instants. In this study, a 1% threshold is employed, meaning convergence is said to occur at time t_c if $\epsilon < 0.01, \forall t \geq t_c$ for all $t \geq t_c$.

Observability is required for successful state reconstruction. The pair (A,C) is observable if and only if the observability matrix $\mathcal{O}$

$$\mathcal{O} = \begin{bmatrix} C \\ CA \\ CA^2 \\ \vdots \\ CA^{n-1} \end{bmatrix} \tag{13}$$

has full rank, where n is the system order. Once observability holds, the desired observer poles $\lambda_1, \lambda_2, \cdots, \lambda_n$ are chosen so that the characteristic polynomial of the error dynamics is:

$$\det\big(sI - (A - L_o C)\big) = (s - \lambda_1)(s - \lambda_2)\cdots(s - \lambda_n) \tag{14}$$

A common guideline is to place the observer poles five to ten times faster than the dominant plant poles; for example, repeated real poles (e.g., $\lambda_1 = \lambda_2 = -\alpha$) yield a critically damped, rapidly convergent response.

4 OBSERVER DESIGN FOR THE BUCK CONVERTER

The Luenberger observer design entails verifying observability, selecting suitable observer poles, and computing the gain matrix L_o. This enables estimation of unmeasurable states from the measurable output voltage.

4.1 Verification of Observability

The first step in the observer design is to verify observability. Using the parameter set in Table 1, the state and output matrices are obtained as:

$$A = \begin{bmatrix} 0 & -\frac{1}{L} \\ \frac{1}{C} & -\frac{1}{RC} \end{bmatrix} = \begin{bmatrix} 0 & -1000 \\ 10000 & -2000 \end{bmatrix}, \qquad C = [\,0 \quad 1\,] \tag{15}$$

Thus, the observability matrix $\mathcal{O}$ is obtained as:

$$\mathcal{O} = \begin{bmatrix} C \\ CA \end{bmatrix} = \begin{bmatrix} 0 & 1 \\ \frac{1}{C} & -\frac{1}{RC} \end{bmatrix} = \begin{bmatrix} 0 & 1 \\ 10000 & -2000 \end{bmatrix} \tag{16}$$

The rank of $\mathcal{O}$ is 2, so the system is observable and observer design can proceed.

Table 1. The Parameters for Buck Converter

L (H)	C (F)	R (Ω)	v_{in} (V)	v_{out} (V)	T_s (µs)
1×10^{-3}	100×10^{-6}	5	40	20	10

4.2 Calculation of the Observer Gain Matrix L_o

Observer pole placement critically determines the convergence of the estimation error. To obtain fast, non-oscillatory behavior, real negative observer poles are selected and placed approximately ten times faster than the dominant plant poles. The plant poles are computed from the following characteristic equation:

$$\det(sI - A) = 0 \tag{17}$$

Substituting the state matrix A from (15) into (17) yields:

$$\det\left(\begin{bmatrix} s & 1000 \\ -10000 & s + 2000 \end{bmatrix}\right) = s^2 + 2000s + 10^7 = 0 \tag{18}$$

Solving the quadratic equation results in the plant poles:

$$s_{1,2} = -1000 \pm j3000 \tag{19}$$

Thus, the system has a pair of complex conjugate poles located at $-1000 \pm j3000$. According to the design guideline, the observer poles are placed ten times faster than the real part of the system poles as follows:

$$\lambda_{1,2} = 10 \times \mathbb{R}(s_{1,2}) = -10000 \tag{20}$$

Therefore, the observer poles are placed at $\lambda_1 = \lambda_2 = -10000$, corresponding to two identical real poles located significantly further left in the complex plane. The observer gain matrix L_o can be determined by equating the characteristic equation of the observer dynamics to the desired characteristic equation.

Let the observer gain be:

$$L_o = \begin{bmatrix} l_1 \\ l_2 \end{bmatrix} \tag{21}$$

The characteristic equation of the observer dynamics can be written as:

$$\det(sI - (A - L_o C)) = 0 \tag{22}$$

Expanding and simplifying the determinant yields the characteristic polynomial:

$$s^2 + (2000 + l_2)s + (10^7 + 10^4 l_1) = 0 \tag{23}$$

The desired characteristic equation for double real poles at $\lambda_{1,2} = -10000$ is:

$$(s + 10000)^2 = s^2 + 2 \cdot 10^4 s + 10^8 \tag{24}$$

Matching the coefficients of (23) and (24) yields:

$$10^7 + 10^4 l_1 = 10^8 \tag{25}$$

$$2000 + l_2 = 2 \cdot 10^4 \tag{26}$$

Solving for l_1 and l_2 gives:

$$L_o = \begin{bmatrix} l_1 \\ l_2 \end{bmatrix} = \begin{bmatrix} 9000 \\ 18000 \end{bmatrix} \tag{27}$$

The observer gain matrix L_o calculated analytically coincides with the matrix obtained via the MATLAB's acker command, confirming the validity of the analytical design process.

5 SIMULATION RESULTS

In this study, the dynamic performance of the Luenberger observer designed for the buck converter was investigated under two different observer pole placements: one with poles identical to the natural poles of system, and another with poles placed ten times farther into the left-half complex plane to achieve faster convergence. The simulations were carried out under nominal operating conditions, with constant input voltage and load resistance, to evaluate the step response of the state variables. Furthermore, the robustness of the observer was assessed under varying input voltage and load resistance, where its ability to accurately track the true system states was examined. To validate the effectiveness of the proposed observer design, time-domain simulations were performed in MATLAB using the average state-space model of the buck converter.

The converter configuration shown in Figure 1(a) was implemented based on the component values summarized in Table I, and the overall plant-observer structure is illustrated in Figure 3. As shown in the control diagram, the observer was integrated into the plant model to estimate unmeasured states. Its dynamic performance, including convergence time and estimation accuracy, is evaluated through the simulation plots presented in Figures 4 to 9. The system dynamics were simulated using a fixed-step Euler integration method with a time step of 10 µs.

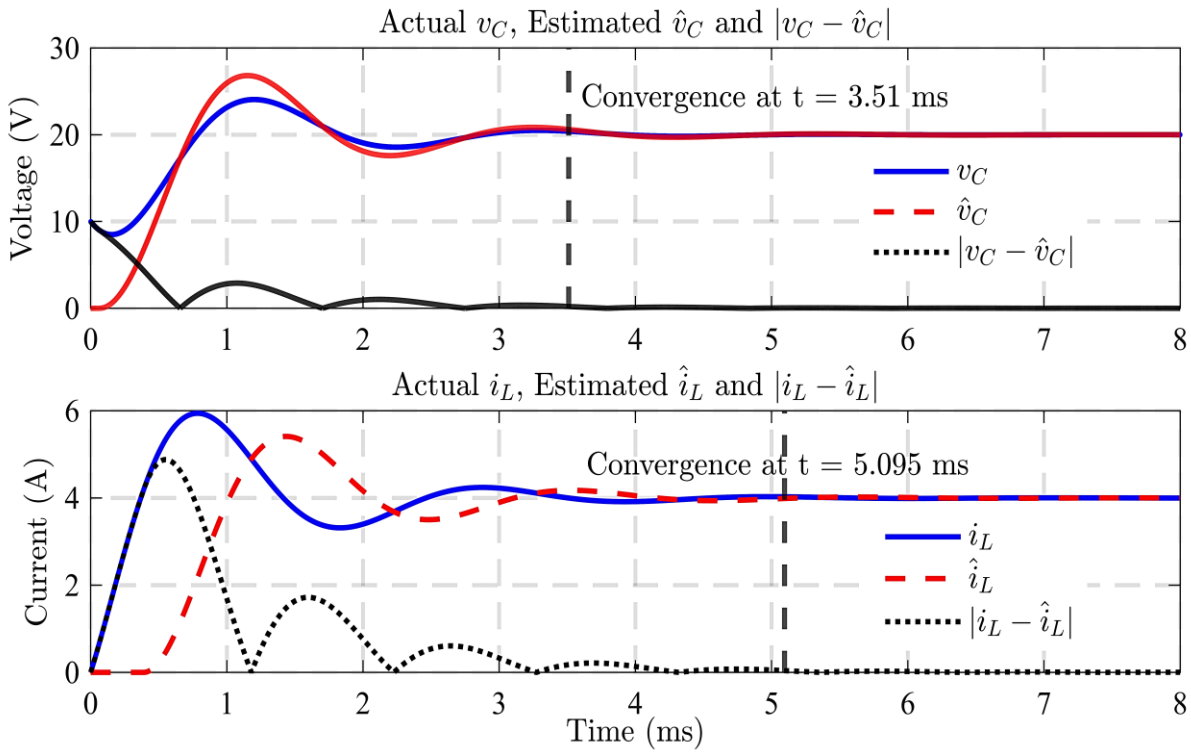


Figure 4. System and observer with the natural pole placement responses under nominal operating conditions (v_{in} = 40 V) with $v_c(0)$ = 10 V. Estimation error drops below 1% at 3.51 ms for v_c and 5.095 ms for i_L.

In nominal operating voltage (v_{in} = 40 V) with $v_c(0)$ = 10 V, the system responses with natural and aggressive observer pole placements are presented in Figures 4 and 5, respectively. In Figure 4, the convergence error of the capacitor voltage and inductor current falls below the 1% threshold at 3.51 ms and 5.095 ms, respectively. In contrast, Figure 5 demonstrates significantly faster convergence, with the errors for the capacitor voltage and inductor current falling below the threshold at 0.409 ms and 0.479 ms, respectively. This disparity highlights the direct influence of observer pole placement speed on the convergence time of the system. In nominal load conditions (R = 5 Ω) with $v_c(0)$ = 15 V, the impact of abrupt changes in source voltage on the system and observer is analyzed in Figures 6 and 7. In this scenario, the input voltage is set to 40 V from 0–8 ms, reduced to 35 V from 8–16 ms, and returned to 40 V from 16–25 ms. Figure 6 illustrates the system behavior with a slow observer using the natural pole placement method. The convergence errors of the capacitor voltage and inductor current drop below the threshold at 3.711 ms and 5.294 ms, respectively.

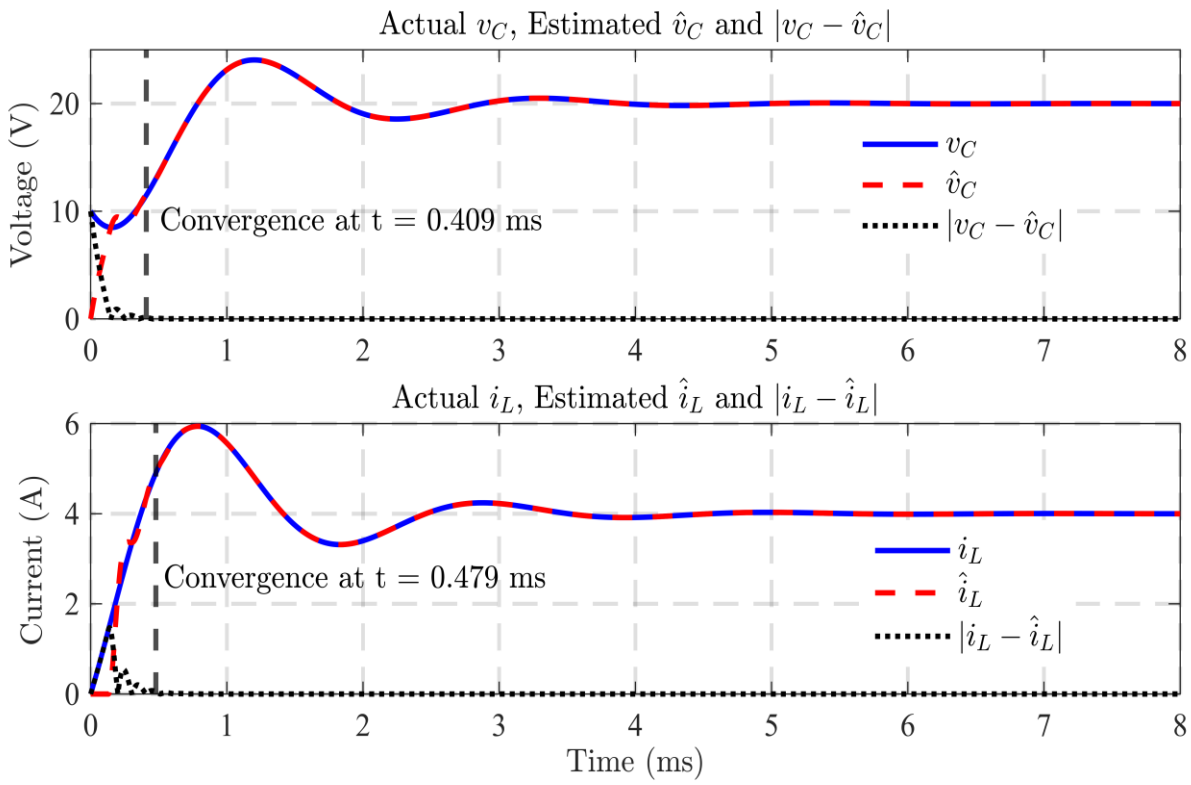


Figure 5. System and observer with aggressive pole placement responses under nominal operating conditions (V_{in} = 40 V) with $v_c(0) = 10\,V$. Faster convergence achieved: 0.409 ms (v_c) and 0.479 ms (i_L), with estimation error <1%.

Despite the step changes in input voltage, the observer continues to track the system dynamics effectively and maintains stable performance. On the other hand, Figure 7 demonstrates that the fast observer, using the aggressive pole placement method, achieves significantly shorter convergence times, with the capacitor voltage and inductor current errors dropping below the threshold at 0.381 ms and 0.524 ms, respectively. The zoomed-in region (0–0.7 ms) clearly shows the rapid settling behavior of the observer. These findings confirm that while the aggressive pole placement method significantly affects the dynamic response of the observer, changes in the input voltage do not negatively impact the performance of the observer. In nominal input voltage ($v_{in} = 40$ V) with $v_c(0) = 20\,V$, the effects of abrupt changes in load resistance on the system and observer behavior are depicted in Figures 8 and 9. The load is set to R = 5 Ω for 0–12 ms, R = 10 Ω for 12–23 ms, and returns to R = 5 Ω for 23–30 ms. Figure 8 shows the performance of the slow observer. The estimated capacitor voltage $\hat{v}_c$ converges to the actual v_c at 3.863 ms, and the estimated inductor current $\hat{i}_L$ converges to the actual i_L at 5.445 ms. The observer successfully reaches steady-state and continues to track system variables despite load changes.

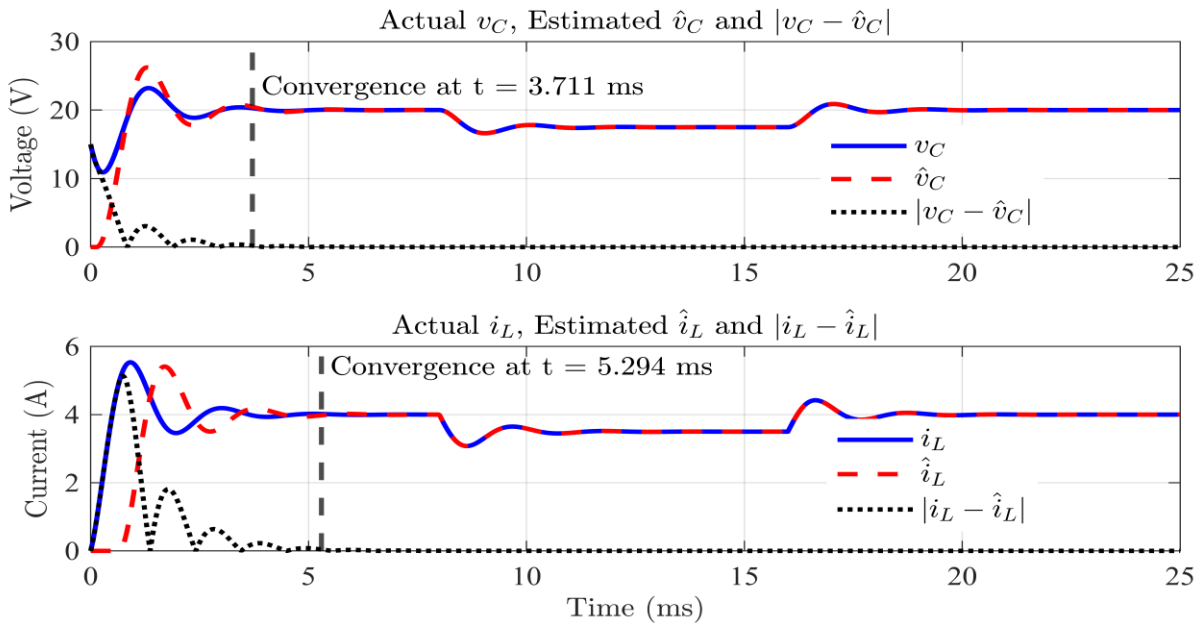


Figure 6. System and observer with natural pole placement responses under nominal load conditions (R=5 Ω) with $v_c(0) = 15\ V$ during sudden changes in input voltage. Estimation error drops below 1% at 3.711 ms (v_c) and 5.294 ms (i_L).

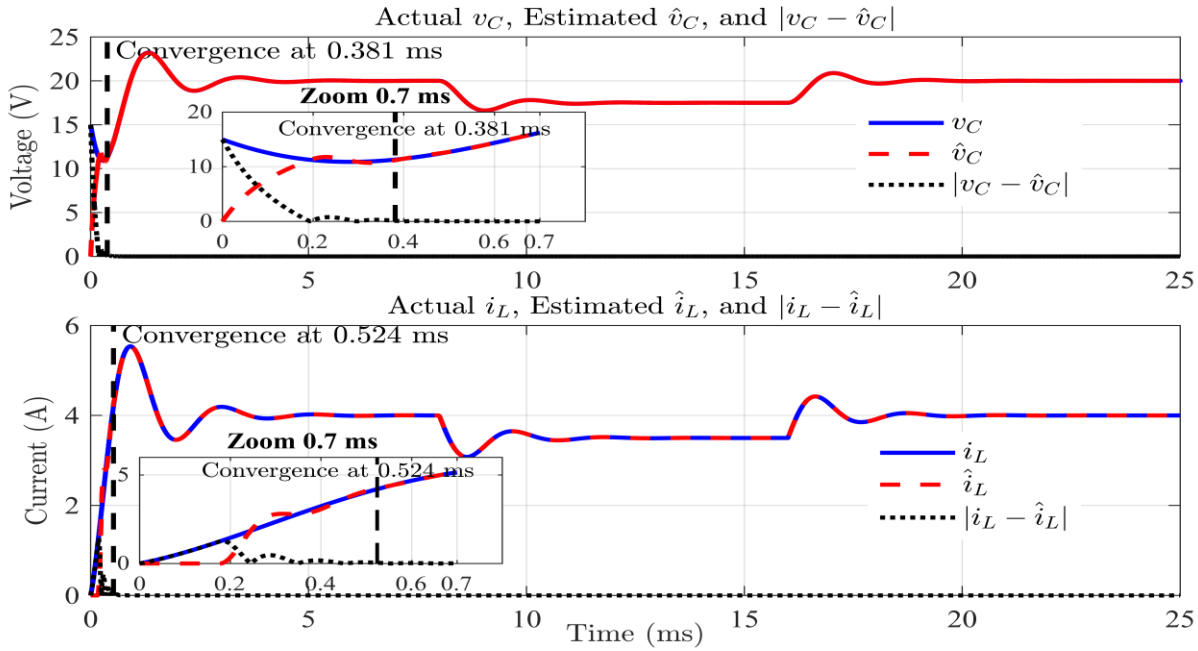


Figure 7. System and observer with aggressive pole placement responses under nominal load conditions (R = 5 Ω) with $v_c(0) = 15\ V$ during sudden changes in input voltage. Faster convergence: 0.381 ms (v_c), 0.524 ms (i_L).

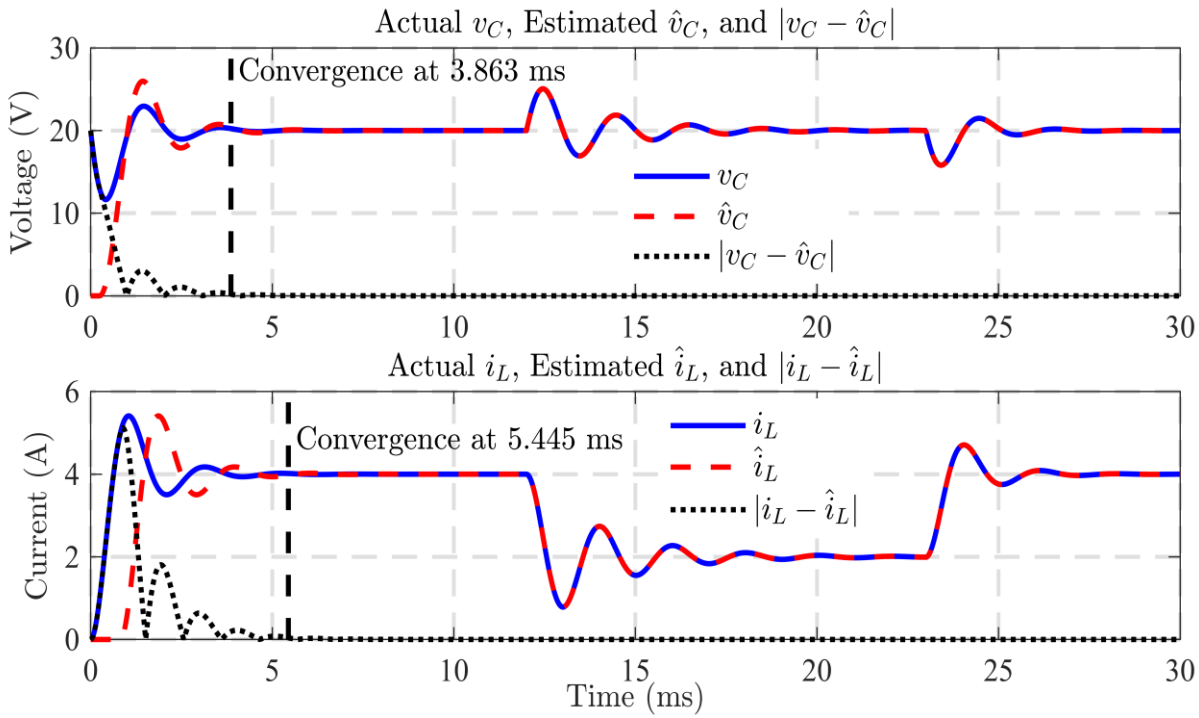


Figure 8. System and observer with natural pole placement responses during sudden load changes (R = 5 Ω to 10 Ω and back to 5 Ω), with constant input voltage ($v_{in} = 40$ V) and $v_c(0) = 20$ V. Estimation error drops below 1% at 3.863 ms (v_c) and 5.445 ms (i_L).

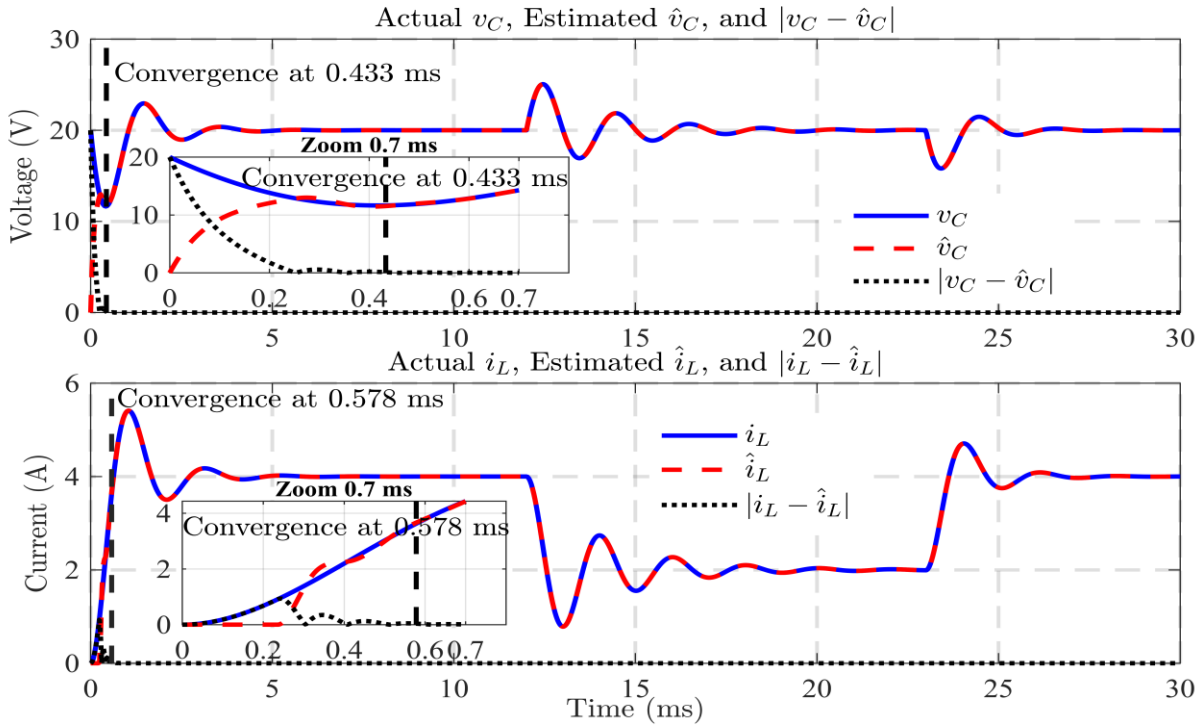


Figure 9. System and observer with aggressive pole placement responses during sudden load changes (R = 5 Ω to 10 Ω and back to 5 Ω), with constant input voltage (V_{in} = 40V) and $v_c(0) = 20$ V. Estimation error drops below 1% at 0.433 ms (v_c) and 0.578 ms (i_L).

Figure 9, on the other hand, presents the response of the fast observer. Here, $\hat{i}_L$ and $\hat{v}_c$ converge to their actual counterparts at 0.578 ms and 0.433 ms, respectively. These results demonstrate that the aggressive pole placement speed plays a critical role in determining the dynamic response time of the observer, while load variations do not significantly affect the performance of observer.

Table 2 presents the convergence times of the observer for both natural and aggressive pole placement under different initial capacitor voltages. The table compares how quickly the estimated capacitor voltage $\hat{v}_c$ and inductor current $\hat{i}_L$ converge to their true values. Results clearly indicate that the aggressive pole placement strategy shortens convergence times dramatically compared to natural pole placement, even when the initial conditions vary. Table 3 summarizes the observer's transient performance, presenting rise time, delay time, overshoot, and steady-state error values under different initial capacitor voltages. These results should be interpreted not as primary performance indicators but as complementary to the convergence analysis. In all cases, the aggressive pole placement yields shorter delay times for both estimated signals, demonstrating that the observer responds more promptly to system changes. While aggressive pole placement results in a shorter rise time for the estimated inductor current $\hat{i}_L$, indicating faster tracking, it causes a slightly longer rise time for the estimated capacitor voltage $\hat{v}_c$. This distinct behavior represents a trade-off that provides a smoother and less abrupt voltage estimate. Overshoot is consistently lower with the aggressive placement, and the steady-state error remains approximately zero for both observer designs, confirming that the estimates converge accurately under all tested conditions.

Table 2. Convergence times of natural and aggressive pole placement under different initial capacitor voltages

Initial Condition	Method	Convergence time for $\hat{v}_c$ (ms)	Convergence time for $\hat{i}_L$ (ms)
$v_c(0) = 10\ V$	Natural	3.51	5.095
	Aggressive	0.409	0.479
$v_c(0) = 15\ V$	Natural	3.711	5.294
	Aggressive	0.381	0.524
$v_c(0) = 20\ V$	Natural	3.863	5.445
	Aggressive	0.433	0.578

Table 3. Rise time, delay time, overshoot, and steady-state error for the observer's estimated capacitor voltage ($\hat{v}_c$) and inductor current ($\hat{i}_L$) under different initial capacitor voltages

Initial Condition	Method	Signal	Rise Time (ms)	Delay Time (ms)	Overshoot (%)	Steady-State Error (%)
$v_c(0) = 10\ V$	Natural	$\hat{v}_c$	0.445	0.474	34.10	0.03
		$\hat{i}_L$	0.423	0.765	35.32	0.08
	Aggressive	$\hat{v}_c$	0.663	0.336	20.28	0.01
		$\hat{i}_L$	0.32	0.17	48.53	0.03
$v_c(0) = 15\ V$	Natural	$\hat{v}_c$	0.49	0.593	31.12	0.02
		$\hat{i}_L$	0.424	1.027	35.27	0.07
	Aggressive	$\hat{v}_c$	0.775	0.156	16.05	0.02
		$\hat{i}_L$	0.244	0.250	38.44	0.04
$v_c(0) = 20\ V$	Natural	$\hat{v}_c$	0.510	0.723	29.9	0.02
		$\hat{i}_L$	0.424	0.194	35.26	0.07
	Aggressive	$\hat{v}_c$	0.905	0.118	25.31	0.01
		$\hat{i}_L$	0.303	0.337	35.25	0.02

6 CONCLUSION

This study has presented a comprehensive analysis of a Luenberger observer designed for the buck converter using an aggressive pole placement strategy. The observer's performance was evaluated under various scenarios, including different pole placement methods, load variations, and input voltage disturbances. By placing the observer poles approximately ten times faster than the natural poles of the system, both the capacitor voltage and inductor current reach their nominal values much more rapidly. Compared to the natural placement, a roughly 10 fold improvement in convergence time was observed. Moreover, the observer exhibited robust performance under sudden input voltage disturbances and time-varying load conditions. This indicates that aggressive pole placement not only enhances the dynamic response but also reduces the observer's sensitivity to external disturbances. Even when the initial conditions of the state variables were different from zero, the proposed observer maintained stability and provided accurate estimations. This further reinforces the reliability and flexibility of the design for real-world applications. All analyses were carried out in MATLAB, and the findings have been presented in detail. Simulation results have demonstrated that the aggressive pole placement approach significantly improves the convergence time of the observer. Compared to previous studies that utilize conventional pole placement techniques for observer-based current estimation, this study provides a distinctive and detailed analysis of the dynamic effects of aggressive pole placement. In the existing literature, observer poles are generally selected to

match the system poles; however, when the state variables start from different initial conditions, this conventional approach results in increased convergence time. By placing the observer poles more aggressively in the left half-plane, this study demonstrates that convergence is significantly accelerated even under mismatched initial conditions, supported by a quantitative comparison of behavior under various operating scenarios. In conclusion, the study confirms that aggressive pole placement provides substantial performance advantages for buck converter observers, offering a fast and reliable state estimation method. As a direction for future work, the proposed observer can be implemented and validated in a real-time HIL or FPGA-based environment to assess its practical performance, latency effects, and robustness under real-world disturbances. Moreover, the observer design can be extended to other converter topologies, such as Boost, Buck-Boost, or Cuk converters. Incorporating adaptive or intelligent pole placement strategies, possibly using optimization or machine learning techniques, could further enhance estimation accuracy and adaptability in dynamically varying systems.

Statement of Research and Publication Ethics

The study is complied with research and publication ethics.

Artificial Intelligence (AI) Contribution Statement

This manuscript was entirely written, edited, analyzed, and prepared without the assistance of any artificial intelligence (AI) tools. All content, including text, data analysis, and figures, was solely generated by the authors.

REFERENCES

[1] F. Evran and M. T. Aydemir, "Isolated High Step-Up DC–DC Converter With Low Voltage Stress," in *IEEE Transactions on Power Electronics*, vol. 29, no. 7, pp. 3591-3603, July 2014.

[2] F. Evran and M. T. Aydemir, “Z-source-based isolated high step-up converter,” *IET Power Electronics*, vol. 6, no. 1, pp. 117–124, 2013.

[3] F. Evran, “Grid-connected inverter,” *Düzce Üniversitesi Bilim ve Teknoloji Dergisi*, vol. 6, no. 4, pp. 1420–1429, 2018.

[4] V. Nicolau, “On PID controller design by combining pole placement technique with symmetrical optimum criterion,” *Mathematical Problems in Engineering*, vol. 2013, no. 1, Art. no. 316827, 2013.

[5] S. Das, K. Halder and A. Gupta, "Delay Handling Method in Dominant Pole Placement Based PID Controller Design," in *IEEE Transactions on Industrial Informatics*, vol. 16, no. 2, pp. 980-991, Feb. 2020.

[6] Z. Wang, S. Li and Q. Li, "Continuous Nonsingular Terminal Sliding Mode Control of DC–DC Boost Converters Subject to Time-Varying Disturbances," in *IEEE Transactions on Circuits and Systems II: Express Briefs*, vol. 67, no. 11, pp. 2552-2556, Nov. 2020.

[7] C. -Y. Chan, "Adaptive Sliding-Mode Control of a Novel Buck-Boost Converter Based on Zeta Converter," in *IEEE Transactions on Circuits and Systems II: Express Briefs*, vol. 69, no. 3, pp. 1307-1311, March 2022.

[8] H. Komurcugil, S. Biricik and N. Guler, "Indirect Sliding Mode Control for DC–DC SEPIC Converters," in *IEEE Transactions on Industrial Informatics*, vol. 16, no. 6, pp. 4099-4108, June 2020.

[9] F. Evran, "Azaltan DA-DA dönüştürücüsü için kayma kip denetleyici tasarımı," *Düzce Üniversitesi Bilim ve Teknoloji Dergisi*, vol. 7, no. 1, pp. 519–530, 2019.

[10] C. Zheng, T. Dragičević, J. Zhang, R. Chen and F. Blaabjerg, "Composite Robust Quasi-Sliding Mode Control of DC–DC Buck Converter With Constant Power Loads," in *IEEE Journal of Emerging and Selected Topics in Power Electronics*, vol. 9, no. 2, pp. 1455-1464, April 2021.

[11] F. Evran, "Azaltan ve yükselten DA–DA dönüştürücüleri için tek çevrim denetleyici tasarımı," *Düzce Üniversitesi Bilim ve Teknoloji Dergisi*, vol. 7, no. 1, pp. 757–768, 2019.

[12] J. Fei and D. Jiang, "Fuzzy Neural Network Sliding-Mode Controller for DC-DC Buck Converter," in *IEEE Internet of Things Journal*, vol. 11, no. 19, pp. 31575-31586, 1 Oct.1, 2024.

[13] P. Mattavelli, L. Rossetto, G. Spiazzi and P. Tenti, "General-purpose fuzzy controller for DC-DC converters," in *IEEE Transactions on Power Electronics*, vol. 12, no. 1, pp. 79-86, Jan. 1997.

[14] B. Ullah, H. Ullah and S. Khalid, "Direct Model Predictive Control of Noninverting Buck-boost DC-DC Converter," in *CES Transactions on Electrical Machines and Systems*, vol. 6, no. 3, pp. 332-339, September 2022.

[15] O. Babayomi, Z. Zhang and Z. Li, "Model-Free Predictive Control of DC–DC Boost Converters: Sensor Noise Suppression With Hybrid Extended State Observers," in *IEEE Transactions on Power Electronics*, vol. 39, no. 1, pp. 245-259, Jan. 2024.

[16] J. K. Banda, D. D. S. Mota and E. Tedeschi, "A Physics-Informed Scaling Method for Power Electronic Converters in Power Hardware-in-the-Loop Test Beds," in *IEEE Open Journal of Industry Applications*, vol. 5, pp. 1-14, 2024.

[17] Kyo-Beum Lee and F. Blaabjerg, "Reduced-order extended luenberger observer based sensorless vector control driven by matrix converter with nonlinearity compensation," in *IEEE Transactions on Industrial Electronics*, vol. 53, no. 1, pp. 66-75, Feb. 2006.

[18] H. Renaudineau, J. -P. Martin, B. Nahid-Mobarakeh and S. Pierfederici, "DC–DC Converters Dynamic Modeling With State Observer-Based Parameter Estimation," in *IEEE Transactions on Power Electronics*, vol. 30, no. 6, pp. 3356-3363, June 2015.

[19] N. N. Nam, N. -D. Nguyen and Y. I. Lee, "Model Predictive Control for a Voltage Sensorless Grid-Connected Inverter With LCL Filter Using Lumped Disturbance Observer," in *IEEE Journal of Emerging and Selected Topics in Power Electronics*, vol. 11, no. 3, pp. 3050-3063, June 2023.

[20] P. Pal, R. K. Behera and U. R. Muduli, "Eliminating Current Sensor Dependencies in DAB Converters Using a Luenberger Observer-Based Hybrid Approach," in *IEEE Transactions on Industry Applications*, vol. 60, no. 4, pp. 6380-6392, July-Aug. 2024.

[21] G. Li, J. He and X. Liu, "A DC Voltage Robust Control Strategy of Boost Converter Based on Load Impedance and Input Voltage Observation," in *IEEE Transactions on Industrial Informatics*, vol. 20, no. 5, pp. 7947-7956, May 2024.

[22] S. K. Pandey, S. L. Patil, U. M. Chaskar and S. B. Phadke, "State and Disturbance Observer-Based Integral Sliding Mode Controlled Boost DC–DC Converters," in *IEEE Transactions on Circuits and Systems II: Express Briefs*, vol. 66, no. 9, pp. 1567-1571, Sept. 2019.

[23] X. Lin, J. Liu, F. Liu, Z. Liu, Y. Gao and G. Sun, "Fractional-Order Sliding Mode Approach of Buck Converters With Mismatched Disturbances," in *IEEE Transactions on Circuits and Systems I: Regular Papers*, vol. 68, no. 9, pp. 3890-3900, Sept. 2021.

[24] S. Rout and S. Das, "Online State-of-Charge Estimation of Lithium-Ion Battery Using a Fault Tolerant and Noise Immune Threefold Modified Adaptive Extended Kalman Filter," in *IEEE Transactions on Transportation Electrification*, vol. 10, no. 4, pp. 9366-9380, Dec. 2024.

[25] M. Abdolahi, J. Adabi and S. Y. M. Mousavi, "An Adaptive Extended Kalman Filter With Passivity-Based Control for DC-DC Converter in DC Microgrids Supplying Constant Power Loads," in *IEEE Transactions on Industrial Electronics*, vol. 71, no. 5, pp. 4873-4882, May 2024.

[26] A. Barros, E. Peretti, D. Fabroni, D. Carrera, P. Fragneto and G. Boracchi, "Adaptive Extended Kalman Filtering for Battery State of Charge Estimation on STM32," in *IEEE Embedded Systems Letters*, vol. 17, no. 3, pp. 160-163, June 2025.